Halogen and Hydrogen Bonding Benzothiophene Diol Derivatives: A Study Using ab initio Calculations and X-Ray Crystal Structure Measurements

Enzo Cadoni,*[a] Giulio Ferino,[a] Patrizia Pitzanti,[a] Francesco Secci,[a] Claudia Fattuoni,[a] Francesco Nicolò,[b] and Giuseppe Bruno*[b]

The aim of this study is to describe and compare the supramolecular interactions, in the solid state, of chloro-, bromo-, and iodobenzothiophene diols. The compounds were obtained through organo-catalyzed reactions starting from 3-substituted halobenzothiophene carbaldehydes. Energies of the noncovalent interactions were obtained by density functional theory calculations. Bond distances and angles were found to be in accordance with those determined by X-ray structure analysis.

anti-Bromobenzothiophene derivatives showed strong halogen···π interactions between bromine and the heterocyclic phenyl ring, corresponding to an energy of 7.5 kcal mol⁻¹. syn-Bromo and syn-iodo derivatives appeared to be isostructural, showing X···O (carbonyl) interactions, π stacking, and formation of extended hydrogen bonding networks. In contrast, the chloro derivatives displayed no halogen bonding interactions.

Introduction

Intermolecular interactions are of fundamental importance for supramolecular assembly and consequently for the properties of organic and inorganic compounds, in view of their use as technological materials, drugs, or biologically active molecules. Halogen bonding, which is a noncovalent interaction in which a halogen acts as electrophile with respect to heteroatoms or π-bond electrons, has received particular attention among those studying supramolecular interactions. Halogen bonding was discovered in the 19th century; its study was resumed in the 1940s by Benasi and Hildebrand,[1] and then rationalized by Hassel[2] during the 1970s. However, it has only been within the last two decades that halogen–heteroatom interactions have received significant attention, as demonstrated by the growing number of publications on this topic.[3] The nature of the halogen bond and the forces involved have been investigated by several research groups.[4] The halogen bond interaction is highly directional and can be rationalized by the presence of a region of positive electrostatic potential known as the σ-hole, centered along the R–X axis on the outermost portion of the halogen surface. The main driving forces that govern this kind of attraction are of electrostatic nature, yet dispersive-type forces, polarization, and charge transfer are also involved. It is well known that the ratio between the electrostatic component and the dispersive forces increases with the electrostatic potential of the σ-hole, which in turn increases proportionally with size of the halogen atom.[5] Furthermore, the electrostatic component increases along with the electronegativity of the atoms or groups bound to the halogen atom.[6] However, several researchers[7,8] argue that in halogen···π systems the dispersion interaction should be the dominant source of attraction between the halogen and the aromatic unit. In addition, charge-transfer interactions seem to contribute to the stabilization of the examined species, as reported by Lu and co-workers.[8] Halogen bonding interactions are typically investigated with two different approaches. The first approach is based on statistical analysis of the distribution of intermolecular distances and the corresponding halogen–heteroatom or halogen···π system angles in data from the Cambridge Structural Database (CSD)[9] and the Protein Data Bank (PDB).[3k] The interaction is effective if the intermolecular halogen–nucleophile distances are shorter than the van der Waals radii and the corresponding angles are optimal. In the second approach, the interaction energies, distances, and angles are generally rationalized by calculations. A survey of the PDB[10] regarding halogen interactions in various biologically active molecules showed that structures with halogen–oxygen interactions slightly outnumber those with halogen···π

[a] Prof. E. Cadoni, Dr. G. Ferino, Dr. P. Pitzanti, Dr. F. Secci, Dr. C. Fattuoni
Dipartimento di Scienze Chimiche
Università degli Studi di Cagliari
Cittadella Universitaria di Monserrato
SS 554, Bivio per Sestu, 90042 Monserrato (CA) (Italy)
E-mail: ecadoni@unica.it

[b] Prof. F. Nicolò, Prof. G. Bruno
Dipartimento di Scienze Chimiche
Università degli Studi di Messina
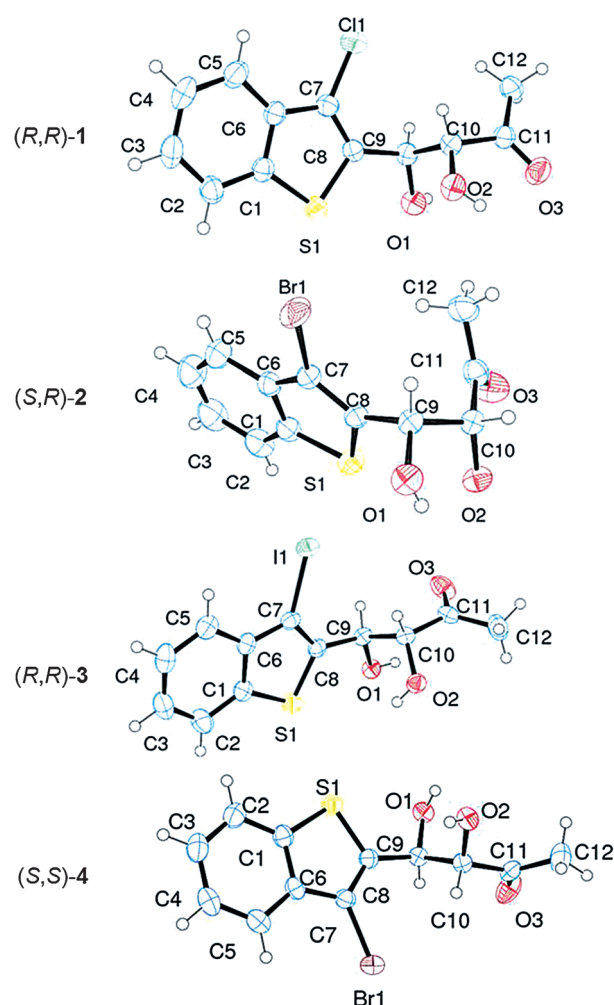Salita Sperone 31, Villaggio S. Agata, 98166 Messina (Italy)
E-mail: gbruno@unime.it

interactions. This is due to the fact that halogen···π aromatic system interactions require a specific geometry in which the carbon–halogen bond must be nearly perpendicular to the aromatic ring, which is not always easy to achieve. However, interaction energies of the halogen···π system calculated on small models such as PhX···Ph are similar in magnitude to those of conventional halogen···O/N bonds.[10] Herein we report the study of several benzothiophene-containing supramolecular structures that were generated by crystallization of various enantiomerically enriched or racemic benzothiophene diols. Particular attention was devoted to analysis of the different inter- and intramolecular interactions, such as hydrogen bonding, π–π stacking, and halogen bonding networks, observed in the crystal structures. Crystallographic measurements were also compared with density functional theory (DFT) calculations in order to assess the energy of such interactions. The role of halogen bonding in determining the crystal packing in highly functionalized molecules was also investigated.

Results and Discussion

Compounds **1**, **2**, and **4** were synthesized by organo-catalyzed aldol reactions using freshly prepared 3-substituted halogen 2-benzothiophene carbaldehydes and hydroxyacetone in the presence of L-proline phenylsulfonamide, as previously described.[11] Compound **3** was prepared in a similar manner by starting from the corresponding 3-iodoaldehyde, as described in the Experimental Section below. After purification, enantiomerically enriched diols were submitted to crystallization in order to obtain pure diastereomeric compounds. Diols **1** and **2** crystallize in centrosymmetric space groups P2₁/n and Pbca, respectively, whereas compound **3** crystallizes in the polar P2₁2₁2₁ space group. Unit cell configurations are racemic mixtures in R,R and S,S for compound **1** and R,S and S,R for **2**. Compound **3** was isolated as enantiomerically pure enantiomer with Flack parameter [0009 (20)], confirming the R,R absolute configuration.

Figure 1 shows that compounds **1** and **3**, as well as the previously elucidated[11] compound **4**, have the same relative *syn* configuration, differing only for the halogen atom substitution at the 3-position, whereas compound **2** has a relative *anti* configuration. For comparison, selected structural data for compounds **1–4** are listed in Tables 1 and 2. Bond distances and angles are similar between the four diols, except for the C–X distances (Table 1). However, pronounced differences among these compounds are observed in the torsion angles of the aliphatic chain. These differences are mainly due to the intermolecular interactions that determine the overall molecular packing.

Torsion angles for pure enantiomeric 3-iodo compound are equal (within one degree) to the corresponding value observed for the isomorphic bromo derivative, where the small difference in cell parameters is essentially due to the different atomic radii of the halogen atoms (Table 2). Intramolecular structural parameters do not need further comments. On the other hand, the molecular packing of these compounds is very pe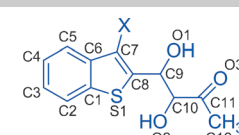culiar, and specific comments for each derivative are reported separately below. Single-crystal X-ray analysis of compounds **1–4** revealed the presence of interactions, as detailed in the following sections.

Figure 1. X-ray crystal structures of compounds **1–4**: ORTEP images of compounds (R,R)-syn-**1**, (S,R)-anti-**2**, (R,R)-syn-**3**, and (S,S)-syn-**4**.

Table 1. Interatomic distances [Å] determined by X-ray crystallography for compounds **1–4**.

Distance	Cl [1]	Br [2]	I [3]	Br [4][a]
C7–X	1.732	1.881	2.078	1.877
C6–C7	1.430	1.430	1.430	1.433
S1–C8	1.730	1.739	1.732	1.731
C9–O1	1.415	1.429	1.423	1.427
C10–O2	1.404	1.406	1.405	1.416
C11–O3	1.207	1.205	1.207	1.210
C8–C9	1.503	1.501	1.508	1.499
C9–C10	1.548	1.530	1.527	1.532
C10–C11	1.516	1.518	1.524	1.524
C11–C12	1.493	1.480	1.493	1.490

[a] See Ref. [11].

Table 2. Bond and dihedral angles [°] determined by X-ray crystallography for compounds **1**–**4**.

| Angle	Cl [1]	Br [2]	I [3]	Br [4][a]
C1-S1-C8	91.6	91.7	91.2	91.8
C6-C7-C8	115.5	114.9	114.1	114.6
C6-C7-X	121.7	121.9	122.9	122.5
X-C7-C8	122.8	123.2	122.8	122.8
C8-C9-O1	110.2	111.3	110.5	110.6
C9-C10-O2	110.6	107.5	110.8	110.1
C10-C11-O3	119.1	117.8	120.4	120.4
C7-C8-C9-O1	−167.0	107.6	167.5[a]	168.7
C8-C9-C10-O2	66.4	−75.1	−69.1	−69.4
O2-C10-C11-O3	14.0	−10.2	−149.8	−149.5

[a] See Ref. [11].

## Single-crystal X-ray analysis and ab initio calculations

Compound 1

The solid-state packing analysis for compound **1** clearly shows the absence of any form of halogen bonding, as chlorine has a lower tendency than bromine and iodine to form halogen bonds, particularly if directly bonded to electron-rich heterocyclic systems.[4b, 12] However, the chlorine atom is involved in a series of weak intra- and intermolecular interactions with several hydrogen atoms, as illustrated in Figure 2. Moreover, the energy contribution of these interactions in determining the crystal organization is certainly negligible relative to the observed π-stacking interaction. 3-Chlorobenzothiophene diols show a tendency to form parallel sheets, which, stabilized by π interactions, form ordinated columns directed along the crystallographic b-axis (Figure 2C). In these structures, the thiophene ring moiety is superposed with the benzene ring of another benzothiophene molecule. The calculated average distance between the sheets is in agreement with the experimentally measured value (3.638 Å). The phenyl group of each molecule is involved in two π interactions, acting as acceptor in one case and as H-π donor in the other, as depicted in Figure 2 A,B. Furthermore, four strong hydrogen bonds, formed between each OH group of every molecule, force four different diol molecules to arrange themselves at the vertices of a rhombus, the center of which lies at the inversion centers at 000. The distances between O(1)^I···O(2)^II and O(1)^I···O(2)^IV were measured to be 2.848 and 3.001 Å, respectively. The corresponding angle O(2)^II···O(1)^I···O(2)^IV was measured at 86.48° (Figure 2).

To understand the nature of the solid-state interactions that determine molecular packing, a series of ab initio calculations starting from the molecular geometry obtained by the X-ray structures was carried out. The trend of the energy gap values for π···π and O···O separation distances is reported in Figure 3. The computed energy minimum for the π···π interaction (blue line) is 4.93 kcal mol⁻¹ and occurs at 3.950 Å. The measured distance in the solid state is 3.650 Å, which in Figure 3 would cor-
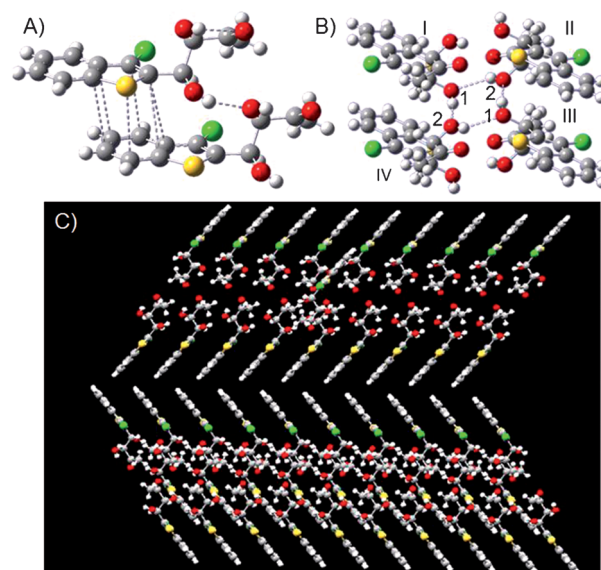
Figure 2. A) Dimeric interactions between two benzothiophene diols of compound **1**: π–π stacking, hydrogen, and chalcogen bonding are displayed as grey dotted lines. B) Hydrogen bond network, depicted as grey dotted lines, between molecules of compound **1** in the tetrameric form. C) Crystal structure packing of compound **1**.
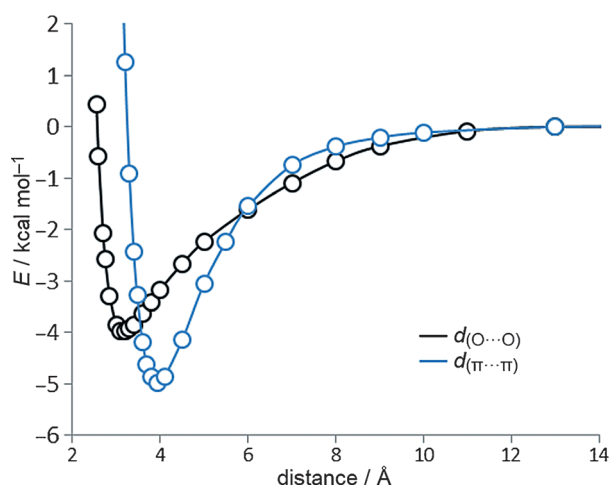
**Figure 3.** Interaction energy diagram of hydrogen bonding (black) and π–π stacking (blue) for compound **1**.

respond to an energy value of 4.13 kcal mol⁻¹. Single-point energy (SPE) calculations for the O···O interaction also reveal that hydrogen bonding interactions between the OH groups provide an energy minimum at 4.00 kcal mol⁻¹, which corresponds to a 3.109 Å O···O distance (black line), slightly higher than the separation distance observed in the solid state (2.848 Å).

Even in this case, the energy difference between the observed and calculated values is 0.80 kcal mol⁻¹. Therefore, it seems that the strong intermolecular hydrogen bonding network between the OH groups drives the supramolecular organization for compound **1**. Weak hydrogen bonding interactions at the inversion center connect two antiparallel supra-

molecular frames, which are also stabilized by π-stacking interactions, finally generating the entire molecular packing (Figure 2C). The intermolecular distance between S1 and the O1 oxygen atom of the overlying benzothiophene molecule is 3.476 Å, which is just above the sum of the van der Waals radii of the two atoms (3.320 Å).

Compound 2

Analysis of compound **2** crystal structures reveal that each molecule is involved in a series of strong attractive hydrogen, halogen, and chalcogen bonding interactions, while π-stacking interactions between the benzothiophene rings are missing (Figure 4 A,B). Within a single molecule, the chalcogen–chalco-
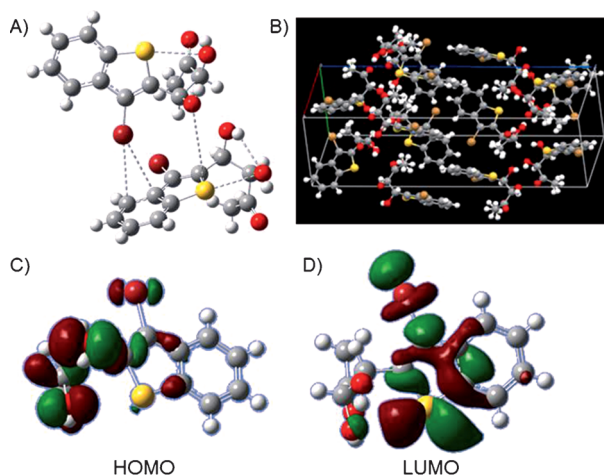

Figure 4. A) Intramolecular S1⋯O2 and intermolecular Br⋯π interactions in compound **2**; bonding interactions are displayed as grey dotted lines. B) Crystal structure packing of compound **2**. C) HOMO Lp–O2 and D) LUMO σ* C1–S1 for the chalcogen intramolecular interaction.

gen interaction involving the sulfur and oxygen atoms S1⋯O2 (3.013 Å) is significantly lower than the sum of their van der Waals radii (3.32 Å). This value is obtained from the interaction between the molecular orbitals (HOMO) of the O2 lone-pair electrons and LUMO σ* S1⋯C1 (Figure 4C,D). To achieve the above interaction, the conformation of the aliphatic chain is heavily distorted, as shown in Figure 4. This causes the aliphatic chain stereogenic carbon atoms to adopt a gauche conformation, favoring the Br⋯π aromatic interactions along the crystal packing. As previously reported by Bruno et al.,[13] S⋯O intramolecular interactions in organosulfur compounds involving both electrostatic and covalent interactions show a wide range of distance values (2.178–3.32 Å), corresponding to the sum of the van der Waals radii, as reported in the CSD.[14]

Analysis of solid-state structural data show that the bond distance between the bromine atom and the main plane containing the aromatic ring of an adjacent 3-bromobenzothiophene diol is 3.427 Å, which is 0.16 Å less than the sum of the van der Waals radii of bromine and the aromatic ring.[15] DFT calculations carried out at the SPE level for this interaction pro-

vided an energy value of 7.53 kcal mol^{-1}. The calculated corresponding distance is in good agreement with the value obtained from the X-ray structure analysis. As shown in Figure 5 A,B, the calculated HOMO and LUMO for two 3-bromobenzothiophene diols reveal that this interaction is not of centroid type, but the bromine atom is directed toward the C4—C5 bond (Figure 5C). Energy calculations for a similar interaction involving a bromo derivative and the C—C axis of a pyridine ring in 4,4′-bipyridine has been reported,[16] providing an energy value of 5.08 kcal mol^{-1} and a Br⋯π (C=C) axis distance of 3.676 Å. Present calculations (Figure 6) give a higher energy
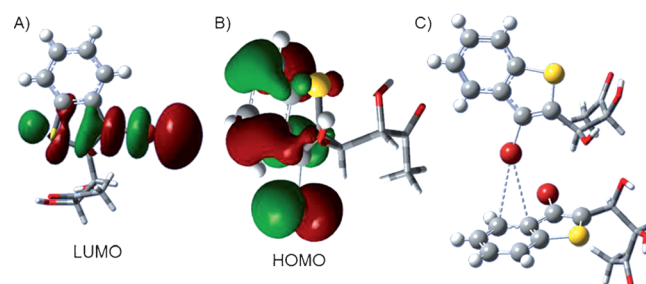
Figure 5. A) LUMO and B) HOMO of the Br⋯π intermolecular interaction. C) Br⋯π (C=C) intermolecular interaction for compound **2**.
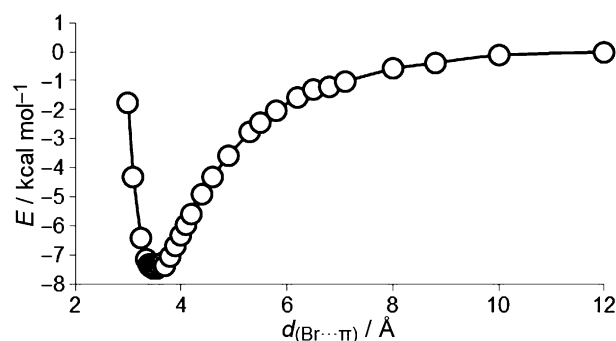
Figure 6. Energy diagram of the Br⋯π interaction for compound **2**.

value of 7.53 kcal mol^{-1}. To the best of our knowledge, only Lu and co-workers[8] obtained similar interaction energy values (8 kcal mol^{-1}) for a benzene-activated Cl–F system, using MP2/aug-cc-PVDZ optimized structures to ensure the stationary geometries. In that case, however, such an energy value is justified, considering the electron-withdrawing effects of the heterocyclic moiety and the related effects on the halogen atom.[17] In contrast, compound **2** has a bromine atom directly bonded to an electron-rich benzothiophene system,[18] which should not increase the bromine's electrophilicity. It can therefore be concluded that the recorded and calculated values for the Br⋯π interaction (7.53 kcal mol^{-1}) is unique for supramolecular structures generated from compound **2**.

Compound 3

3-Iodobenzothiophene diol derivative **3** is isomorphic with compound **4**. X-ray analysis for this compound reveals an

iodine–carbonyl oxygen interaction at 3.115 Å (3), a value 12% lower than the sum of van der Waals radii for the oxygen and iodine atoms (3.500 Å). DFT calculations carried out at the same level for compounds **1** and **2** provided, for 3-iodobenzothiophene diol derivative **3**, an interaction energy value of 8.50 kcal mol^{-1} (Figure 7). This value is in line with the previous
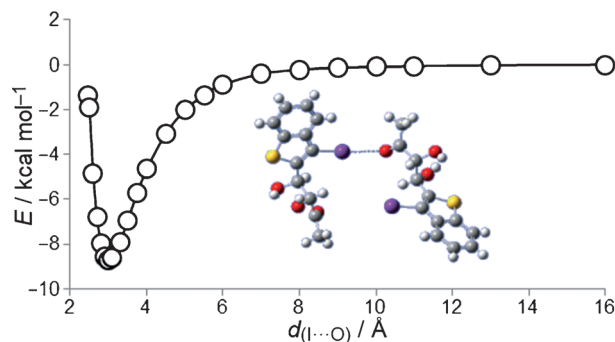

Figure 7. Energy diagram of the I···O interaction for compound **3**.

results obtained for bromine derivative **2**, and is also in agreement with published data.[4b, 6, 10, 19] The halogen bonding strength increases with size of the halogen itself, due to a greater σ-hole, moving from bromine to iodine. Furthermore, solid-state analysis gave angles of 174.08° and 113.54° for C7-I···O3 and carbonyl oxygen O···I, respectively, which is in agreement with the present calculations for this structure. Such angles are optimal in maximizing the halogen bonding between iodine and oxygen, as the σ-hole is directly oriented toward one of the oxygen lone pairs. In addition, the calculations reveal that lengthening of the C7—I bond occurs as a consequence of halogen bonding formation.

X-ray analysis also reveals strong π–π stacking interactions between the benzene ring of a diol unit and the thiophene moiety of a second benzothiophene diol derivative, occurring at of 3.592 Å. The calculated interaction energy (Figure 8) is 5.70 kcal mol^{-1}. The crystal packing is also influenced by the occurrence of hydrogen bonding.

Compound 4

X-ray crystallographic data gathered in determining the absolute configuration of compound **4** were reported previously;[11] the crystal structure packing is shown in Figure 9. No other crystallographic investigations have been published for this diol derivative. Analysis of compound **4** reveals the formation of a noncovalent interaction network involving the halogen atom. Various π–π stacking, hydrogen bonding, and halogen bonding interactions between the bromine and the carbonyl oxygen atom O3 were also observed. An intramolecular chalcogen–chalcogen interaction involving S1—O1 occurs with a distance of 2.889 Å. As observed for compound **2**, the distance between S and O for compound **4** is also smaller than the sum of the van der Waals radii. This is a consequence of the interaction between the lone-pair electrons of the oxygen atom O1
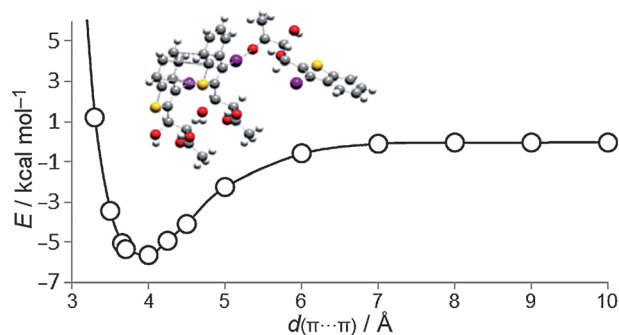

Figure 8. Energy diagram of the π···π interaction for compound **3**.

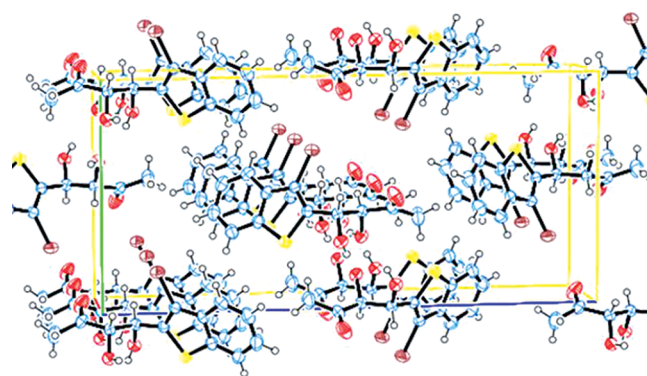**Figure 9.** Crystal structure packing of compound **4**.

and the S1—C1 σ* molecular orbital, which determines the conformation of the aliphatic chain.

DFT calculations provided a Br···O (carbonyl) energy interaction of 2.22 kcal mol^{-1} and a Br···O distance of 3.110 Å, as shown in Figure 10. This distance is in agreement with the X-ray crystallographic data and is lower than the sum of van der Waals radii for oxygen and bromine atoms (3.370 Å). The LUMO and HOMO (Figure 11) of two interacting molecules clearly show that the LUMO is localized on the bromine atom of one molecule, while the HOMO is localized on the carbonyl oxygen atom of the other. The oxygen lone pair faces the bromine σ-hole, confirming the optimum values found for the C=O···Br and C—Br···O angles observed in the crystal structure (110.14° and 171.42°, respectively). To confirm the formation of an intermolecular Br···O bond, calculations were performed, providing a lengthening of the C7—Br bond, as the bimolecular system forms from the single 3-bromobenzothiphene diol **4**. At first sight, the energy corresponding to the C=O···Br and C—Br···O angles that maximize contact between the oxygen lone pair and the bromine σ-hole seems lower than one would expect. However, although the halogen bonding energy increases with the s character of the carbon atom to which the halogen is bound,[20] only strong electron-withdrawing R groups can provide robust interactions.[4e, 18] It can therefore be assumed that the moderately electron-rich properties of benzothiophene decrease the electrophilicity of bromine, explaining this behavior.
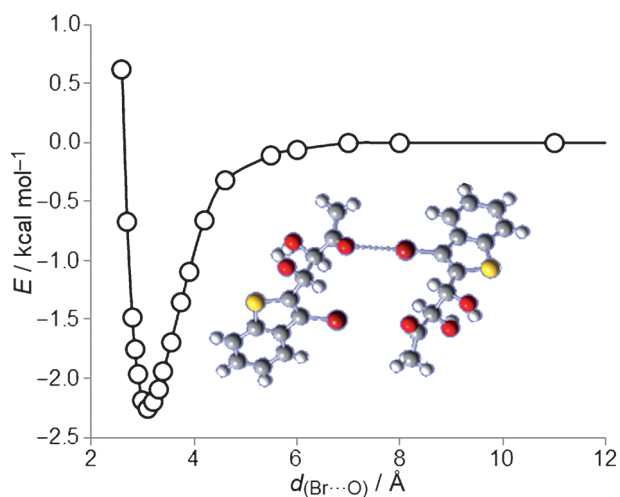
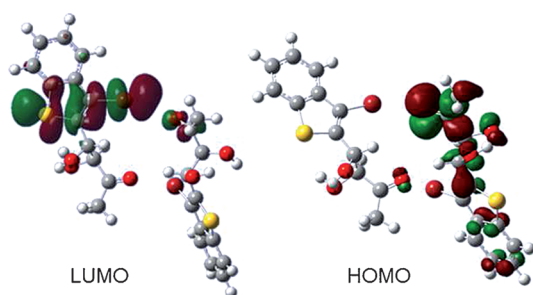**Figure 10.** Energy diagram of the Br···O interaction of compound **4**.

Figure 11. LUMO and HOMO of the Br···O intermolecular interaction for compound **4**.

Comparison of interaction energy values

The range of calculated energy values of halogen bonding is very wide, and many research groups have reported different intervals. Resnati and co-workers[3c] reported energy values that vary between 2.40 and 78 kcal mol^{-1}, whereas an energy range of 3–15 kcal mol^{-1} was observed by Mooibroek and Gamez.[21] According to Zou et al.,[19] the energy range was 0.3–33 kcal mol^{-1}. However, for R–X···O or R–X···π systems, energy values < 10 kcal mol^{-1} are found in the literature, being quite similar for similar R groups. For example, Wallnoefer et al.[7c] obtained an interaction energy value of 3.42 kcal mol^{-1} for the C_6H_5Br···π (p-$CH_3C_6H_4OH$) (acceptor-activated halogen bonding) system by using the MP2/cc-pDVZ method, while Riley et al.[4e] found an interaction energy value of 2.23 kcal mol^{-1} for the C_6H_5Br···O=$C(CH_3)_2$ system using the MP2/aug-cc-pDVZ method. Similar results were obtained for haloethylene or haloethyne with benzene versus haloethylene or haloethyne with NH_3.[20,21] In this work, the study of *syn*- and *anti*-bromine derivatives revealed that despite the C=O···Br (110.14°) and C–Br···O (171.42°) angles being able to maximize the energy value, the energy value for the Br···π aromatic ring interaction is threefold higher than that of the bromine–carbonyl oxygen interaction. The finding that the Br···π interaction is stronger than the Br···O interaction is supported by the calculated

length of the C7–Br bond, also observed in the corresponding crystal structures (Figure 1). The interaction energy value (8.50 kcal mol^{-1}) obtained for I···O in compound **3** is very high, even in comparison with other systems in which iodine is bound to strong electron-attracting aromatic species.[19]

Conclusions

In summary, for all the *syn*-**1**, **3**, and **4** structures investigated in this work there is clear evidence for the formation of a π-staking interaction between the thiophene moiety of a benzothiophene diol molecule and the benzene ring of a second one. In the *anti*-bromo derivative **2** this interaction is absent due to the folding of the alkyl chain resulting from hydrogen bonding between the OH groups and the S–O2 chalcogen interaction. A key point concerning formation of the crystalline structure of the chlorine derivative **1** is represented by the formation of a hydrogen bonding network linking four benzothiophene units. Finally, for all three *syn* stereoisomers **1**, **3**, and **4**, the establishment of π–π interactions results in the formation of benzothiophene pillars linked to each other through halogen or hydrogen bonds. Halogen bonding plays a significant role in determining the crystal packing type for this kind of compound.

Experimental Section

X-ray crystallography data collection and structure refinement: Colorless single crystals of compounds suitable for X-ray structure analysis were selected from the crystals obtained from an ethyl acetate/hexane solution. Data were collected at room temperature with a Bruker APEX II CCD area-detector diffractometer and graphite-monochromatized MoKα radiation [$\lambda = 0.71073$ Å]. Data collection, cell refinement, data reduction and absorption correction by multi-scan methods were performed by programs included in the Bruker software package.[22] Structures were solved by direct methods using XS97. The non-hydrogen atoms were refined anisotropically by the full-matrix least-squares method on F20 using SHELXL97.[23] All hydrogen atoms were introduced in calculated positions and constrained to ride on their parent atoms. The CCDC 1024956, 1024957, and 1024958 contain the supplementary crystallographic data for this paper. These data can be obtained free of charge from the Cambridge Crystallographic Data Centre via www.ccdc.cam.ac.uk/data_request/cif.

Computational methods: All ab initio and DFT calculations were performed with the GAUSSIAN 03 program package.[24] Molecular structures of all compounds were fully optimized at various levels. Geometry optimizations were first carried out at the HF level with the 6-31+G(d,p) basis set and afterward the effect of electron correlation on the molecular geometry was taken into account by using Becke's three-parameter hybrid, and the gradient corrected Lee–Yang–Parr correlational functional (B3LYP)[25] employing the 6-31+G(d,p) basis set. Vibrational frequency calculations were performed at the same level used for geometry optimization.

For iodine compound **3**, Gaussian-type basis set 6-31+G(d,p) was used for the C, O, and H atoms. The quasi-relativistic effective core potential (RECP) SDD and valence basis sets recommended by Andrae et al. were used.[26]

Synthesis and characterization: ^{1}H and ^{13}C NMR spectra were recorded on Varian 500 spectrometer using the solvent peak as internal reference. ESI mass spectra were obtained on a Varian 310-MS LC–MS mass spectrometer, with the atmospheric pressure ionization (API) technique. The sample solutions (10 mg L^{-1}) were prepared in CH$_3$CN and infused directly into the ESI source using a programmable syringe pump, at a flow rate of 1.50 mL h^{-1}. Needle, shield, and detector voltages were kept at 4800, 600, and 1250 V, respectively. Pressure of nebulizing and drying gas was 12 psi, housing and drying gas temperatures were 60 and 50 °C, respectively. Infrared spectra were obtained using a Bruker FTIR instrument. Optical rotation values were measured at 25 °C using a PolAAr32 instrument. Melting points were obtained on a Kofler hot stage microscope. THF was distilled from sodium/benzophenone. Benzothiophene and hydroxyacetone were used as purchased. The diol compound was separated by column chromatography (25×180 mm) using DAVISIL silica gel (40–63 m), packed with Büchi C-670 cartridge.

3-Bromo-1-benzothiophene-2-(2-dioxolanyl): was prepared from 3-Bromo-1-benzothiophene-2-carbaldehyde[11] as described previously.[27]

3-Iodo-1-benzothiophene-2-(2-dioxolanyl): was prepared from 3-Bromo-1-benzothiophene-2-(2-dioxolanyl) according reported methods.[28] To a solution of 3-bromo-1-benzothiophene-2-(2-dioxolanyl) (1.31 g, 4.58 mmol) in Et$_2$O (25 mL) at −78 °C, tBuLi (3.9 mL, 5.5 mmol, 1.2 equiv) was added dropwise. The reaction mixture was stirred for 1 h at the same temperature, and iodine (2.33 g, 9.16 mmol, 2 equiv in 10.0 mL Et$_2$O) was added. The resulting mixture was allowed to warm to room temperature and was treated with aqueous NH$_4$Cl (Saturated, 25 mL). The organic layer was separated, the aqueous layer was extracted with Et$_2$O (3×25 mL), and the ether and organic layers were combined. The combined organic phase was washed with saturated Na$_2$S$_2$O$_3$ (3×20 mL), water (3× 20 mL). The organic phase was dried on Na$_2$SO$_4$ and concentrated. Pure dioxolanyl compound was obtained after flash chromatography using petroleum ether (PE)/EtOAc 90:10 as eluent.

3-Iodo-1-benzothiophene-2-carbaldehyde: A solution of aqueous HClO$_4$ (70% 0.47 mL) in H$_2$O (1.5 mL) was added to a solution of 3-iodo-1-benzothiophene-2-(2-dioxolanyl) (1 g 3.47 mmol) in acetone (50 mL) at room temperature. The resulting mixture was stirred at room temperature for 24 h and then extracted with Et$_2$O (3×20 mL), washed with H$_2$O and dried on Na$_2$SO$_4$. The crude product was purified by flash chromatography using Et$_2$O/PE 1:10 to give the product as red crystals (80% yield). Experimental data are consistent with those reported earlier.[29]

syn-(3R,4R)-4-(3-Iodo-1-benzothiophen-2-yl)-3,4-dihydroxybutan-2-one: To a hydroxyacetone (4.4 mL, 60 mmol, 20 equiv) solution of 1-benzothiophene-2-carbaldehyde (0.5 g, 3.00 mmol) at 0 °C, L-proline (18 mg, 0.070 mmol, 0.1 equiv) was added in one portion. The mixture was stirred for 78 h at this temperature, and the resulting mixture was treated with aqueous NH$_4$Cl (saturated, 15 mL) and extracted with EtOAc (20 mL). The organic phase was dried with Na$_2$SO$_4$ and concentrated under reduced pressure after filtration. The yellow crude solid was subjected to chromatography with PE/CH$_2$Cl$_2$/EtOAc 35:35:20 to afford the corresponding syn-aldol adducts as white solid (needles; 0.4 g, 33% yield); mp: 121.5–122.5 °C; $[\alpha]_D^{25} = -45.4°$ (c=0.65 CHCl$_3$); IR (neat): $\nu = 3443$, 1730 cm^{-1}; ^{1}H NMR (500 MHz, CDCl$_3$): $\delta = 7.81$ (d, 1H, J=8.0 Hz), 7.77 (d, 1H, J=8.0 Hz), 7.46 (t, 1H, J=7.5 Hz), 7.40 (t, 1H, J=7.5 Hz), 5.60 (br d, 1H, J=3.5 Hz), 4.56 (br s, 1H), 3.89 (d, 1H, J=4.5 Hz, D$_2$O, exc), 3.02 (d, 1H, J=6.5 Hz, D$_2$O, exc), 2.43 (s, 3H);

^{13}C NMR (125 MHz, CDCl$_3$): $\delta = 206.2$, 143.1, 140.3, 138.2, 125.8, 125.4, 125.2, 122.6, 110.0, 79.4, 72.8, 25.8; MS (ESI$^+$): m/z (%) = 747 (30) [2M + Na]$^+$, 385 (100) [M + Na]$^+$.

Compounds **1** and **2** were synthesized according to published methods.[11]

Acknowledgements

[1] H. A. Benesi, J. H. Hildebrand, J. Am. Chem. Soc. **1949**, 71, 2703–2707.
[2] O. Hassel, Science **1970**, 170, 497–502.
[3] a) P. Metrangolo, H. Neukirch, T. Pilati, G. Resnati, Acc. Chem. Res. **2005**, 38, 386–395; b) P. Metrangolo, G. Resnati, Science **2008**, 321, 918–919; c) P. Metrangolo, F. Meyer, T. Pilati, G. Resnati, G. Terraneo, Angew. Chem. Int. Ed. **2008**, 47, 6114–6127; Angew. Chem. **2008**, 120, 6206–6220; d) P. Metrangolo, J. S. Murray, T. Pilati, P. Politzer, G. Resnati, G. Terraneo, Cryst. Growth Des. **2011**, 11, 4238–4246; e) L. Meazza, J. A. Foster, K. Fucke, P. Metrangolo, G. Resnati, J. W. Steed, Nat. Chem. **2013**, 5, 42–47; f) A. R. Voth, F. A. Hays, P. S. Ho, Proc. Natl. Acad. Sci. USA **2007**, 104, 6188–6193; g) K. E. Riley, P. Hobza, Cryst. Growth Des. **2011**, 11, 4272–4278; h) P. Auffinger, F. A. Hays, E. Westhof, P. S. Ho, Proc. Natl. Acad. Sci. USA **2004**, 101, 16789–16794; i) H. L. Nguyen, P. N. Horton, M. B. Hursthouse, A. C. Legon, D. W. Bruce, J. Am. Chem. Soc. **2004**, 126, 16–17; j) A. R. Voth, P. Khuu, K. Oishi, P. S. Ho, Nat. Chem. **2009**, 1, 74–79; k) H. Matter, M. Nazaré, S. Güssregen, D. W. Will, H. Schreuder, A. Bauer, M. Urmann, K. Ritter, M. Wagner, V. Wehner, Angew. Chem. Int. Ed. **2009**, 48, 2911–2916; Angew. Chem. **2009**, 121, 2955–2960; l) M. Mazik, A. Hartmann, P. G. Jones, Eur. J. Org. Chem. **2010**, 458–463.
[4] a) T. Clark, M. Hennemann, J. S. Murray, J. S. Politzer, J. Mol. Model. **2007**, 13, 291–296; b) P. Politzer, P. Lane, M. C. Concha, Y. Ma, J. S. Murray, J. Mol. Model. **2007**, 13, 305–311; c) F. A. Bulat, A. Toro-Labbé, T. Brinck, J. S. Murray, P. Politzer, J. Mol. Model. **2010**, 16, 1679–1691; d) P. Politzer, J. S. Murray, T. Clark, Phys. Chem. Chem. Phys. **2010**, 12, 7748–7757; e) K. E. Riley, J. S. Murray, J. Fanfrlík, J. řezáč, R. J. Solá, M. C. Concha, F. M. Ramos, P. Politzer, J. Mol. Model. **2011**, 17, 3309–3318.
[5] K. E. Riley, J. S. Murray, J. Fanfrlík, J. Ř. Ricardo, J. Solá, M. C. Concha, F. M. Ramos, P. Politzer, J. Mol. Model. **2013**, 19, 4651–4659.
[6] K. E. Riley, P. Hobza, J. Chem. Theory Comput. **2008**, 4, 232–242.
[7] a) Y. N. Imai, Y. Inoue, I. Nakanishi, K. Kitaura, Protein Sci. **2008**, 17, 1129–1137; b) Y. N. Imai, Y. Inoue, I. Nakanishi, K. Kitaura, QSAR Comb. Sci. **2009**, 28, 869–873; c) H. G. Wallnoefer, T. Fox, K. R. Liedl, C. S. Tautermann, Phys. Chem. Chem. Phys. **2010**, 12, 14941–14949.
[8] Y. X. Lu, J. W. Zou, Y. H. Wang, Q. S. Yu, Int. J. Quantum Chem. **2007**, 107, 1479–1486.
[9] D. Swierczynski, R. Luboradzki, G. Dolgonos, J. Lipkowski, H. J. Schneider, Eur. J. Org. Chem. **2005**, 1172–1177.
[10] Y. X. Lu, Y. Wang, W. Zhu, Phys. Chem. Chem. Phys. **2010**, 12, 4543–4551.
[11] F. Secci, E. Cadoni, C. Fattuoni, A. Frongia, G. Bruno, F. Nicolo, Tetrahedron **2012**, 68, 4773–4781.
[12] F. F. Awwadi, R. D. Willett, K. A. Peterson, B. Twamley, Chem. Eur. J. **2006**, 12, 8952–8960.
[13] G. Bruno, A. Chimirri, R. Gitto, S. Grasso, F. Nicolo, R. Scopelliti, M. Zappala, J. Chem. Soc. Perkin Trans. 1 **1997**, 2211–2215.
[14] F. H. Allen, C. M. Bird, R. S. Rowland, P. R. Raithby, Acta Crystallogr. Sect. B **1997**, 53, 696–701.
[15] a) O. Hassel, C. Romming, Q. Rev. Chem. Soc. **1962**, 16, 1–18; b) N. Nagels, D. Hauchecorne, W. A. Herrebout, Molecules **2013**, 18, 6829–6851.

[16] V. Mollica Nardo, A. De Robertis, G. Bruno, F. Nicolò, *J. Iran. Chem. Soc.* **2014**, DOI: 10.1007s13738-014-0437-3.

[17] a) T. A. Logothetis, F. Meyer, P. Metrangolo, T. Pilati, G. Resnati, *New J. Chem.* **2004**, *28*, 760–763; b) K. E. Riley, J. S. Murray, P. Politzer, M. C. Concha, P. Hobza, *J. Chem. Theory Comput.* **2009**, *5*, 155–163.

[18] *Heterocyclic Chemistry in Drug Discovery* (Ed.: J. J. Li), Wiley, Hoboken, **2013**, p. 125.

[19] J. W. Zou, Y. J. Jiang, M. Guo, G. X. Hu, B. Zhang, H. C. Liu, Q. S. Yu, *Chem. Eur. J.* **2005**, *11*, 740–751.

[20] Y. X. Lu, J. W. Zou, Y.-H. Wang, Q.-S. Yu, *Chem. Phys.* **2007**, *334*, 1–7.

[21] T. J. Mooibroek, P. Gamez, *CrystEngComm* **2013**, *15*, 4565–4570.

[22] COSMO (ver. 1.60), SAINT (ver. 7.06A), SADABS (ver. 2.10), SHELXS (ver. 97): Bruker AXS, Madison, WI (USA), **2005**.

[23] G. M. Sheldrick, SHELXL97, University of Göttingen, Göttingen (Germany), **1997**.

[24] M. J. Frisch, G. W. Trucks, H. B. Schlegel, P. M. W. Gill, B. G. Johnson, M. A. Robb, J. R. Cheeseman, T. Keith, G. A. Petersson, J. A. Montgomery, K. Raghavachari, M. A. Al-Laham, V. G. Zakrzewski, J. V. Ortiz, J. B. Foresman, J. Cioslowski, B. B. Stefanov, A. Nanayakkara, M. Challacombe, C. Y. Peng, P. Y. Ayala, W. Chen, M. W. Wong, J. L. Andres, E. S. Replogle, R. Gomperts, R. L. Martin, D. J. Fox, J. S. Binkley, D. J. Defrees, J. Baker, J. P. Stewart, M. Head-Gordon, C. Gonzalez, J. A. Pople, GAUSSIAN 03, Gaussian Inc., Pittsburgh, PA (USA), **2003**.

[25] A. D. Becke, *J. Chem. Phys.* **1993**, *98*, 5648–5652.

[26] D. Andrae, U. Häußermann, M. Dolg, H. Stoll, H. Preuβ, *Theor. Chim. Acta* **1990**, *77*, 123–141.

[27] N.-W. Tseng, M. Lautens, *J. org. Chem.* **2009**, *74*, 1809–1811.

[28] T. P. Sura, D. W. H. MacDowel, *J. org. Chem.* **1993**, *58*, 4360–4369.

[29] L. Cuesta, I. Maluenda, T. Soler, R. Navarro, E. P. Urriolabeitia, *Inorg. Chem.* **2011**, *50*, 37–45.